International Journal of Wavelets, Multiresolution
and Information Processing
Vol. 16, No. 1 (2018) 1850009 (17 pages)

DOI: 10.1142/S0219691318500091

World Scientific
www.worldscientific.com

Enhanced discrete wavelet packet sub-band frequency edge detection using Hilbert transform

P. Y. Dibal* and E. N. Onwuka†

Telecommunication Engineering Department
Federal University of Technology, Minna
Niger State, Nigeria
**yoksa77@gmail.com*
†*onwukaliz@futminna.edu.ng*

J. Agajo

Computer Engineering Department
Federal University of Technology, Minna
Niger State, Nigeria
agajojul@gmail.com

C. O. Alenoghena

Telecommunication Engineering Department
Federal University of Technology, Minna
Niger State, Nigeria
carol@futminna.edu.ng

Received 23 July 2017
Accepted 25 October 2017
Published 27 November 2017

The wavelet packet transform as a mathematical tool has found recent application in spectrum sensing. The result of this application has produced very promising results. Primarily, wavelets were designed for edge detection in images. Recently, cognitive radio literature have reported on wavelet application to detect sub-band frequency edges in wide band spectrum. In this paper, we present the combination of the Hilbert transform and the wavelet packet transform with the aim of enhancing the detection of the sub-band frequency edges of a wavelet-packet-decomposed signal. The simulation results show the effectiveness of this approach. The new scheme detected sub-band frequency edges of the wavelet-packet-decomposed signal much better than the wavelet packet transform without combination with the Hilbert transform.

Keywords: Discrete wavelet packet transform; Hilbert transform; frequency edge; local maxima; cognitive radio.

AMS Subject Classification: 22E46, 53C35, 57S20

1. Introduction

Wavelet packets are an extension of the discrete wavelet transform (DWT) with the difference being that while the DWT decomposes only the low-pass frequency component of an input signal, the wavelet packet decomposes both the low-pass frequency and high-pass frequency components of an input signal. This results in the wavelet packets having higher resolution and better fidelity.

Wavelet packets are usually implemented using filter banks, and such an implementation is called a wavelet system, which is defined as the representation of a signal or function by a set of building blocks. Figure 1, called the analysis filter bank, shows the implementation of a wavelet packet using filter banks. For each of the filters in the analysis bank, the filter processes half of the total frequency band of the input signal at that stage.[23]

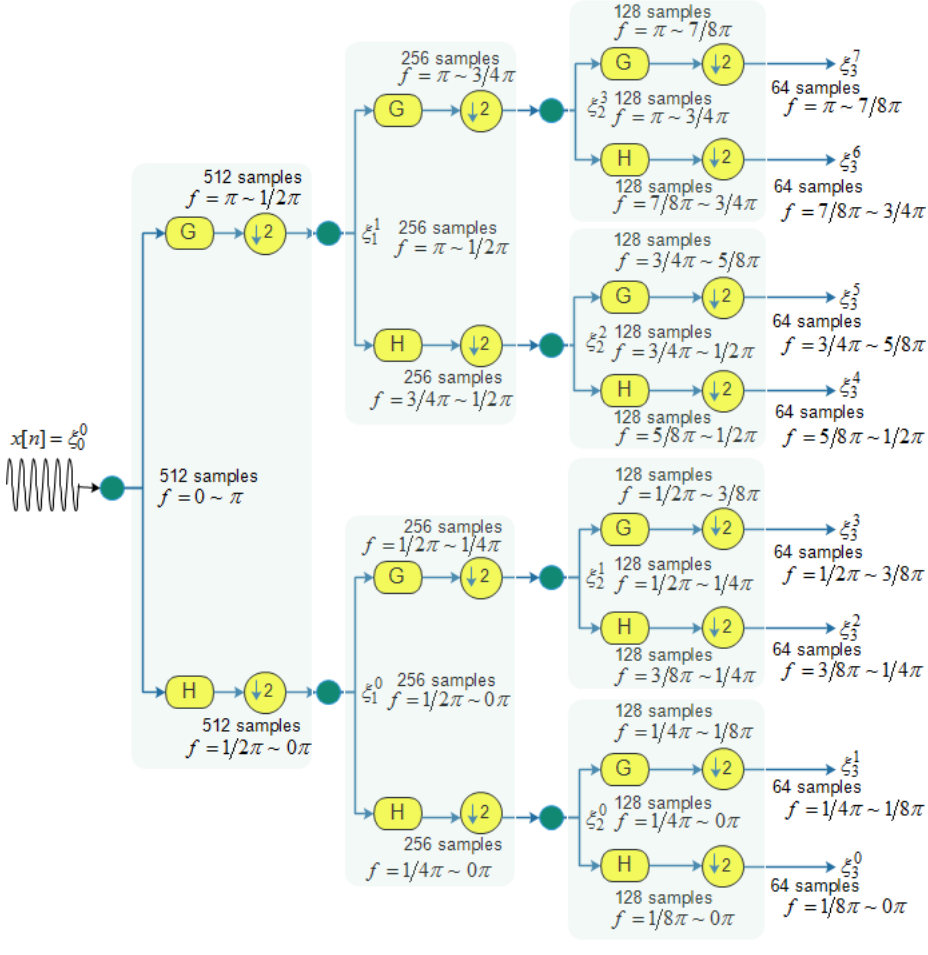

Fig. 1. Analysis filter bank of a wavelet packet.

This paper focuses on the terminal nodes of the analysis part of the filter bank. Each of the terminal nodes of the analysis part of the filter bank outputs frequencies (also called sub-band frequencies) of different range from a decomposed signal. From the structure of the analysis filter bank shown in Fig. 1, the sub-band frequencies occur adjacent to each other. In this paper, the Hilbert transform will be applied to the signals at the terminal nodes of the analysis filter bank in order to achieve improved sub-band frequency edge detection.

2. Brief Theory of Wavelet Detection

An edge is a place of local transitions from one object to another. They are usually not complete borders, and are just locally-identifiable probable transitions. In the analysis of the properties of transient signals like communication signals and vibration signals,[25] edges are viewed as points of sharp variations. Edges can have one dimension or higher dimensions. One-dimensional edges are the focus of this research because the low-pass and high-pass filters in Fig. 1 are one-dimensional. There are different types of one-dimensional edges as depicted in Fig. 2.

The step edge occurs when a signal has sudden and abrupt change in value on one side of a discontinuity or another. The line edge occurs when there is an abrupt change in value, but the signal returns to the starting value within a short interval. The ramp edge occurs in a signal when the change in intensity is not instantaneous; the change usually occurs over a finite distance. The roof edge is similar to the ramp edge, but it is usually generated by the intersection of surfaces.

The points of sharp variations in a signal are identified as either a local maximum, or a local minimum. The local maximum is defined as the highest value in a portion of a given set of points, but not necessarily the highest point in all values of the set. Similarly, the local minimum is defined as the lowest value in a portion of a given set of points, but not necessarily the lowest point in all the values of the set. Local maxima and local minima are the basis of wavelet-based detection of wideband signals, which uses edges (points of sharp variations) in wideband signals to identify the frequency bands that make up the signal spectrum. The methods for detecting edges are briefly introduced below.

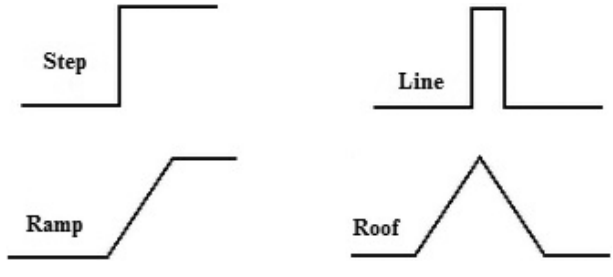

Fig. 2. Types of one-dimensional edges.

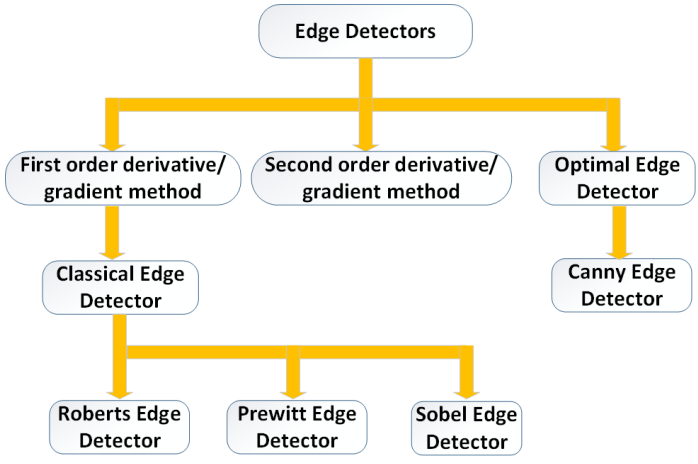

Fig. 3. Classification of edge detection methods.

2.1. *Edge detection methods*

The methods employed in edge detection are broadly categorized into three[7]:

(i) First-order derivative/gradient method
(ii) Second-order derivative method
(iii) Optimal edge detection method.

Figure 3 depicts the classification of these methods of edge detection. The first-order derivative is also called a gradient method, and it makes use of three operators[4,5,13,17,27]: Roberts operator, Prewitt operator, and Sobel operator. Edge determination using the first-order derivative method involves the determination of the minimum and maximum points in a signal through the first-order differential equation of the signal.

The second-order derivative method is also known as the Laplacian method, and it involves locating edges in a signal through the search for zero crossings.[3,22,28]

The third type of edge detector is the optimal edge detector, which makes use of the Canny operator. The Canny operator works by defining edges as zero crossings of second derivatives in the direction of the greatest first derivative.[6] The definition of the edges as zero crossing of the second order derivative is achieved through a multi-stage process which involves the use of a Gaussian convolution to smooth a given signal, and then highlighting the regions of the signal with high spatial derivatives.[12,14,15,18,24]

2.2. *Canny edge detector as a local maxima of a wavelet transform modulus*

According to Ref. 21, the local maxima of a wavelet transform modulus is equivalent to the Canny edge detector. Mathematically, this assertion is presented

as follows:

Definition 2.1. We define a smoothing function $\theta(x)$ (which could be Gaussian) that has an integral of 1, and at infinity it converges to 0. Assume that $\theta(x)$ is differentiable twice, and that $\psi^a(x)$ is the first-order derivative of $\theta(x)$ and $\psi^b(x)$ is the second-order derivative of $\theta(x)$.[21]

From Definition 2.1, $\psi^a(x)$ and $\psi^b(x)$ can be expressed as:

$$\psi^a(x) = \frac{d\theta(x)}{dx} \tag{2.1}$$

$$\psi^b(x) = \frac{d^2\theta(x)}{dx^2} \tag{2.2}$$

Also, from Definition 2.1, we can posit that:

$$\int_{-\infty}^{\infty} \psi^a(x)dx = 0 \quad \text{and} \quad \int_{-\infty}^{\infty} \psi^b(x)dx = 0. \tag{2.3}$$

By (2.3), $\psi^a(x)$ and $\psi^b(x)$ are said to be wavelets since their integral is 0. Given a function $\xi(x)$, we dilate it by a scaling factor s, such that:

$$\xi_s(x) = \frac{1}{s}\xi\left(\frac{1}{s}\right). \tag{2.4}$$

For any signal, the wavelet transform can be obtained by the convolution of the signal with the dilated wavelet. Hence, this implies that given the wavelet $\psi^a(x)$ defined in (2.3), the wavelet transform of the function $f(x)$ at the scale s and position x can be calculated as:

$$w_s^a f(x) = f^* \psi_s^a(x). \tag{2.5}$$

Similarly,

$$w_s^b f(x) = f^* \psi_s^b(x). \tag{2.6}$$

Substituting $\psi^a(x)$ and $\psi^b(x)$ from (2.1) and (2.2) into (2.5) and (2.6) yields:

$$w_s^a f(x) = f * \left(s\frac{d\theta_s}{dx}\right) x = s\frac{d}{dx}(f * \theta_s)(x) \tag{2.7}$$

$$w_s^b f(x) = f * \left(s^2\frac{d^2\theta_s}{dx^2}\right) x = s^2\frac{d^2}{dx^2}(f * \theta_s)(x) \tag{2.8}$$

$w_s^a f(x)$ in (2.7) is the wavelet transform of $f(x)$ of the first-order derivative smoothed at a scale s, and $w_s^b f(x)$ in (2.8) is the wavelet transform of the second-order derivative also smoothed at a scale s.

By the classification of edge detection methods shown in Fig. 3, the local extrema of $w_s^a f(x)$ (since it is a first-order derivative method) corresponds to the zero crossings of $w_s^b f(x)$ (since it is a second-order derivative method), and inflection points of $f * \theta_s$. When $\theta(x)$ is Gaussian, the extrema detection corresponds to Canny edge

detection.[8] A large value of the scale s guarantees that the convolution with $\theta_s(x)$ removes small fluctuations.

The operation $f * \theta_s$ yields an inflection point which could either be a maximum or minimum of the absolute value of its first-order derivative. Sharp variation points are identified by the maxima of the absolute value of the first-order derivative, and slow variations are identified by the minima of the absolute value.[18] Hence, the points of sharp variations or edges can be identified and selected by detecting the local maxima of the wavelet transform of $f(x)$ i.e.

$$\hat{x}_n = \max_x |w_s^a f(x)|. \tag{2.9}$$

Equation (2.9) is the basis by which wavelet achieves edge detection in a wide-band signal spectrum.

3. Brief Review of Hilbert Transform

The Hilbert transform is a technique used in signal analysis, and has application in different fields of science and engineering including the detection and diagnosis of faults,[10] gear box fault diagnosis,[26] QRS-wave detection in biomedical engineering.[2] The major advantage of the Hilbert transform over other transforms is that it does not require any change in domain for its operation.[1] Given a real valued signal $x(t)$, the Hilbert transform of such a signal is defined as the convolution of $x(t)$ with $1/\pi t$. The parameter $1/\pi t$ is defined as the kernel of the Hilbert transformer. Mathematically, the Hilbert transform of $x(t)$ can be expressed as[9]:

$$y(t) = h(t) * x(t) = \frac{1}{\pi t} x(t) \tag{3.1}$$

$$y(t) = \frac{1}{\pi} \int_{-\infty}^{\infty} x(\tau) \frac{1}{t-\tau} d\tau = -\frac{1}{\pi} \int_{-\infty}^{\infty} x(\tau) \frac{1}{\tau - t} d\tau, \tag{3.2}$$

where $h(t)$ is the Hilbert transformer. The coupling at $t = \tau$ is possible owing to the Cauchy principal value of the integral. The summation of $x(t)$ and its Hilbert transform forms an analytic signal, which is expressed as:

$$z(t) = x(t) + iy(t). \tag{3.3}$$

In polar notation (3.3) can be expressed as:

$$z(t) = A(t)e^{i\phi(t)}, \tag{3.4}$$

where

$$A(t) = \sqrt{x^2(t) + y^2(t)} \quad \text{and} \quad \phi(t) = \tan^{-1}\left[\frac{y(t)}{x(t)}\right]. \tag{3.5}$$

In (3.5), $A(t)$ represents the instantaneous amplitude, and $\phi(t)$ represents the instantaneous phase of the analytic signal respectively. The rate of change of the

instantaneous phase is defined as instantaneous frequency.[20] Hence:

$$w(t) = \phi'(t) = \frac{d}{dt}\phi(t), \tag{3.6}$$

where $w(t)$ is the instantaneous frequency.

The instantaneous frequency (IF) is a very important concept in communication. Given the spectrum of a signal, instantaneous frequency can be used to obtain the differences in the local phase of the signal (since it is the derivative of a phase), and at the same time detect variations in frequency of the given spectrum. This property of instantaneous frequency makes it better in the detection of edges (frequency variation points) in a signal spectrum, than the constant frequency method used in the Fourier transform (Fourier transform assumes the frequency of a spectrum is constant). Furthermore, owing to its ability to detect the differences in the local phase of a signal, it outperforms power amplitude method and power spectrum method in side channel analysis.[16]

4. Instantaneous Frequency Spread

Given an instantaneous frequency (IF), its spread σ_{IF}^2 is defined as[11]:

$$\sigma_{\mathrm{IF}}^2 = \int [\varphi'(t) - \langle w_i \rangle]^2 |s(t)|^2 dt, \tag{4.1}$$

where $s(t)$ is the signal, $\varphi'(t)$ is derivative of phase, and $\langle w_i \rangle$ is the average weight at i.

If we assume that the average instantaneous frequency is the mean frequency, i.e. $\langle w_i \rangle = \langle w \rangle$, then (4.1) becomes:

$$\sigma_{\mathrm{IF}}^2 = \int [\varphi'(t) - \langle w \rangle]^2 |s(t)|^2 dt. \tag{4.2}$$

Let the bandwidth of a signal be defined as[11]:

$$B^2 = \int \left[\frac{A'(t)}{A(t)}\right]^2 A^2(t) dt + \int [\varphi'(t) - \langle w \rangle]^2 A(t)^2 dt, \tag{4.3}$$

where A is the amplitude.

In (4.3), the bandwidth is an average of two terms, with one depending on the amplitude, and the other depending on the phase. A comparison between (4.2) and (4.3) shows that the second term on the right in (4.3) is actually (4.2). Hence, (4.3) can be rewritten as:

$$B^2 = \sigma_{\mathrm{IF}}^2 + \int \left[\frac{A'(t)}{A(t)}\right]^2 A^2(t) dt. \tag{4.4}$$

Since the second term on the right in (4.4) is positive, then it implies that:

$$B^2 - \int \left[\frac{A'(t)}{A(t)}\right]^2 A^2(t) dt = \sigma_{\mathrm{IF}}^2. \tag{4.5}$$

From (4.5), it can be seen that the spread of the instantaneous frequency will always be smaller than the bandwidth of the signal i.e.:

$$\sigma_{\mathrm{IF}} \leq B. \tag{4.6}$$

The implication of (4.6) is that since the spread of the instantaneous frequency is smaller than the bandwidth of the signal under consideration, then the instantaneous frequency can detect variations in frequency of a given signal spectrum which occur at the edges (boundary) of different frequency bandwidth; and it can be used easily to obtain differences in the local phase of the signal.

5. Application of Hilbert Transform to Discrete Wavelet Packet Transform

To improve the edge detection of the wavelet packet, we consider a wide-band signal characterized by consecutive bands B_n, having power spectrum density (PSD) that is piecewise smooth, as shown in Fig. 4.

The signal spectrum shown in Fig. 4 is characterized by the following:

(i) The location of the spectrum bands is between f_0 and f_N
(ii) An nth band is defined as: $B_n : \{f \epsilon B_n : f_{n-1} \leq f \leq f_n\}, n = 1, 2, \ldots, N$
(iii) For the nth band, the center frequency is defined as: $f_{c,n} = \frac{f_{n+1}+f_n}{2}$.

The structure of the PSD in Fig. 4 is such that in the wide-band spectrum under consideration whose frequency bandwidth spans f_0 to f_N, there are signals whose frequency bandwidth span a finite length f_{N-1} to f_n within the bandwidth of the spectrum. These signals have frequency edges called sub-band frequency edges which mark their starting point and ending point. The sub-band frequency edges can be detected by the discrete wavelet packet transform (DWPT) technique. However, subjecting the DWPT to a Hilbert transform, which is the focus of this section, will yield better results owing to the properties of the Hilbert transform described in Sec. 3.

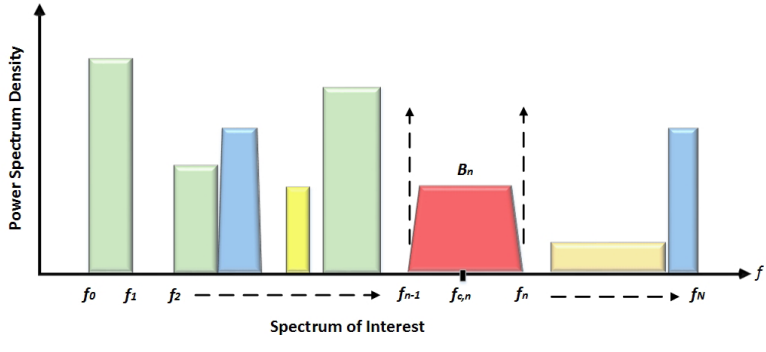

Fig. 4. Spectrum of interest.

If the received power is $S_r(f)$, then by (2.9):

$$\hat{x}_n = \max_x |w_s^a s_r(f)|. \tag{5.1}$$

According to Ref. 19, the wavelet packets in Fig. 1 perform wavelet packet transform decomposition on a signal by the set of recursion equations:

$$\xi_{l+1}^{2p}[n] = \sqrt{2}\sum_k h[k]\xi_l^p[2n-k], \quad n = 0, 1, 2, \ldots, N, \tag{5.2}$$

where $\xi_{l+1}^{2p}[n]$ are the wavelet packet coefficients generated using the scaling filter, $h[k]$ is the low-pass filter, and p is the node at level l of the recursion.

$$\xi_{l+1}^{2p+1}[n] = \sqrt{2}\sum_k g[k]\xi_l^p[2n-k], \quad n = 0, 1, 2, \ldots, N, \tag{5.3}$$

where $\xi_{l+1}^{2p}[n]$ are the wavelet packet coefficients generated using the scaling filter, $g[k]$ is the high-pass filter, and p is the node at level l of the recursion.

Applying (5.2) and (5.3) to (2.9) yields the following set of equations:

$$\hat{x}_{n_h} = \max_n |\xi_{l+1}^{2p}[n]| = \max_n \left|\sqrt{2}\sum_k h[k]\xi_l^p[2n-k]\right|, \quad n = 0, 1, 2, \ldots, N \tag{5.4}$$

$$\hat{x}_{n_g} = \max_n |\xi_{l+1}^{2p+1}[n]| = \max_n \left|\sqrt{2}\sum_k g[k]\xi_l^p[2n-k]\right|, \quad n = 0, 1, 2, \ldots, N, \tag{5.5}$$

where $\hat{x}_{n_h}$ is the local maximum obtained for the lowpass filter $h[k]$ at level l and node p in a given wavelet packet filter bank. Similarly $\hat{x}_{n_g}$ is the local maximum obtained for the highpass filter $g[k]$ at level l and node p in a given wavelet packet filter bank. This local maximum for $\xi_{l+1}^{2p}[n]$ and $\xi_{l+1}^{2p+1}[n]$ clearly identifies the boundary for each sub-band piecewise PSD at different levels of decomposition for the signal.

From the Hilbert transform defined in (3.2), (5.4) and (5.5) can be written as:

$$y_h(m) = -\frac{1}{\pi}P\int_{-\infty}^{\infty}\frac{\xi_{l+1}^{2p}[n]}{n-m}dn, \quad n = 0, 1, 2, \ldots, N \tag{5.6}$$

$$y_h(m) = -\frac{1}{\pi}P\int_{-\infty}^{\infty}\frac{\sqrt{2}\sum_k h[k]\xi_l^p[2n-k]}{n-m}dn, \quad n = 0, 1, 2, \ldots, N \tag{5.7}$$

$$y_g(m) = -\frac{1}{\pi}P\int_{-\infty}^{\infty}\frac{\xi_{l+1}^{2p+1}[n]}{n-m}dn, \quad n = 0, 1, 2, \ldots, N \tag{5.8}$$

$$y_g(m) = -\frac{1}{\pi}P\int_{-\infty}^{\infty}\frac{\sqrt{2}\sum_k g[k]\xi_l^p[2n-k]}{n-m}dn, \quad n = 0, 1, 2, \ldots, N. \tag{5.9}$$

Equations (5.7) and (5.9) yield the Hilbert transform of the local maximum produced by the wavelet packet transform $\xi_{l+1}^{2p}[n]$ and $\xi_{l+1}^{2p+1}[n]$ at the sub-band

edges, which is the point of interest. The Hilbert transform of the local maximum will detect subtle changes in the instantaneous frequency because by (4.6), the spread of the instantaneous frequency derived from the Hilbert transform is always less than the bandwidth under consideration.

6. Simulation and Results

Using simulation, (5.7) and (5.9) were verified for a wavelet packet with level-5 decomposition. The simulation is set up under the conditions described in Table 1. For this paper, level-5 decomposition is considered in the decomposition of the input signal. This level of decomposition is considered ideal because it gives a fine level of resolution of the input signal, and any level higher than this does not necessarily improve accuracy. Figure 5 shows the wavelet packet tree for level-5 decomposition.

At SNR of -15 dB, the input signal to the wavelet packet tree is shown in Fig. 6.

There are 32 channels obtained after level-5 decomposition of the input signal. Investigation of the matrix used to represent the coefficients in each channel shown in Fig. 7 reveals that there are 22 coefficients (usually determined by the sampling rate) in each channel of the terminal nodes of the wavelet packet tree.

The pattern of the distribution of these coefficients in each channel at -15 dB is shown in Fig. 8.

Figure 9 shows the PSD from channel 0 to channel 7, alongside its Hilbert transform. The edge between channels 1 and 2 is amplified. It can be seen that while the wavelet transform poorly identifies this edge (point 44 on x-axis), the application

Table 1. Experimental set-up parameters.

	Amplitude	Frequency(Hz)
SIGNAL 1	1.3	15
SIGNAL 2	1.7	40
SIGNAL 3	2.0	67
SIGNAL 4	1.8	81

Note: SNR $= -15$ dB, -10 dB, 0, 10 dB.

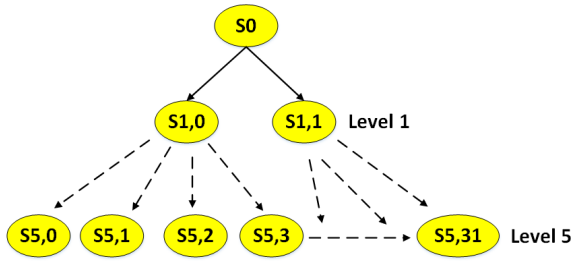

Fig. 5. Wavelet packet tree for level-5 decomposition.

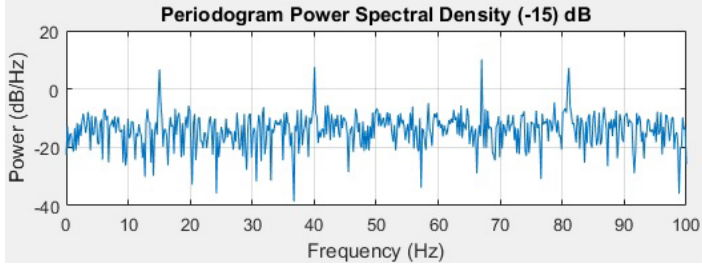

Fig. 6. Periodogram of input signal at −15 dB.

Fig. 7. A 22 × 32 matrix generated from terminal nodes of wavelet packet tree.

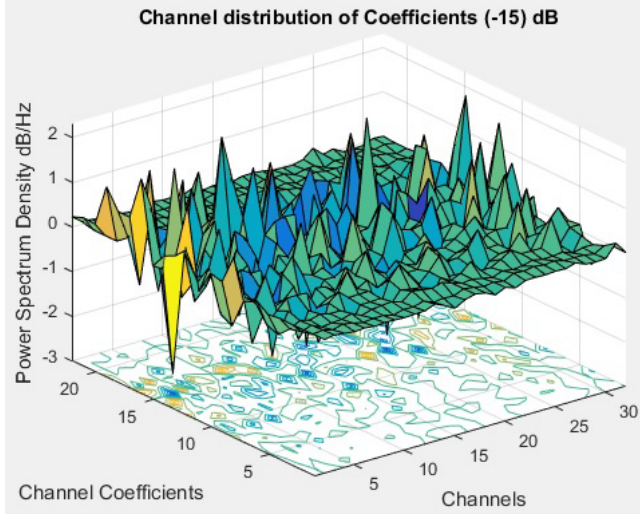

Fig. 8. Distribution pattern of coefficients in each channel at −15 dB.

of the Hilbert transform gives an improved detection of the edge due to the instantaneous frequency being able to identify subtle changes in the phase of a signal.

Similarly, Figs. 10–12 show the PSD of the DWPT with the HT version and a zoomed-in edge of different groups channels. In each case, it could be seen that the HT has an appreciable enhancement on the detection of the edges.

Figures 13–16 show a comparison between the sub-band frequency edge detection made by the discrete wavelet packet transform (DWPT) and the Hilbert transform of the DWPT for all the 32 channels in the terminal nodes at SNR values of −15 dB, 10 dB, 0 dB and 10 dB, respectively. It can be seen that the application of

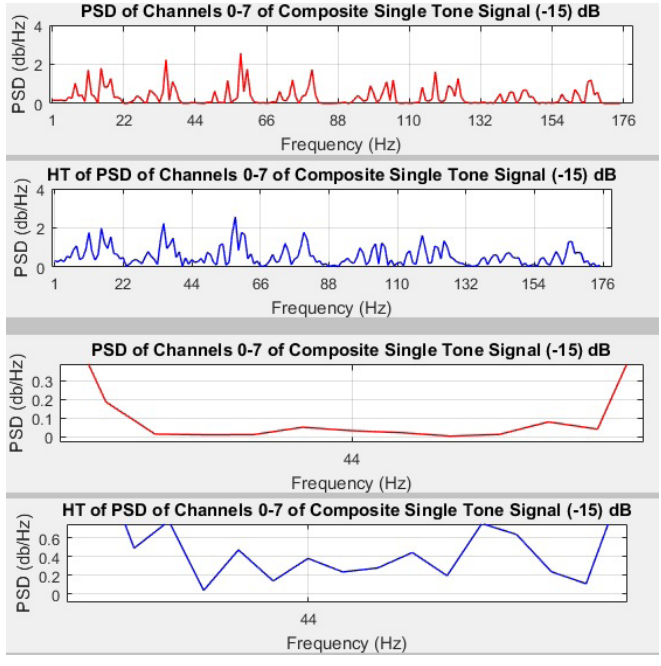

Fig. 9. PSD of channels 0 to 7 at −15 dB, with corresponding Hilbert transform.

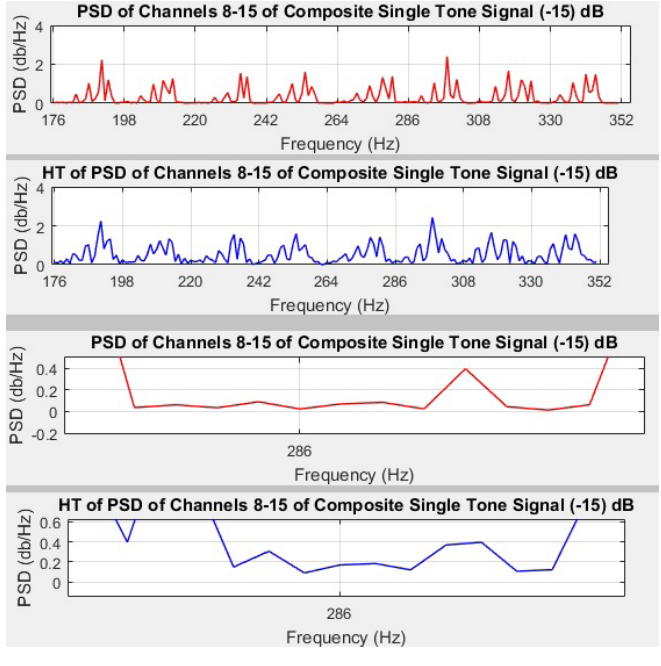

Fig. 10. PSD of channels 8 to 15 at −15 dB, with corresponding Hilbert transform.

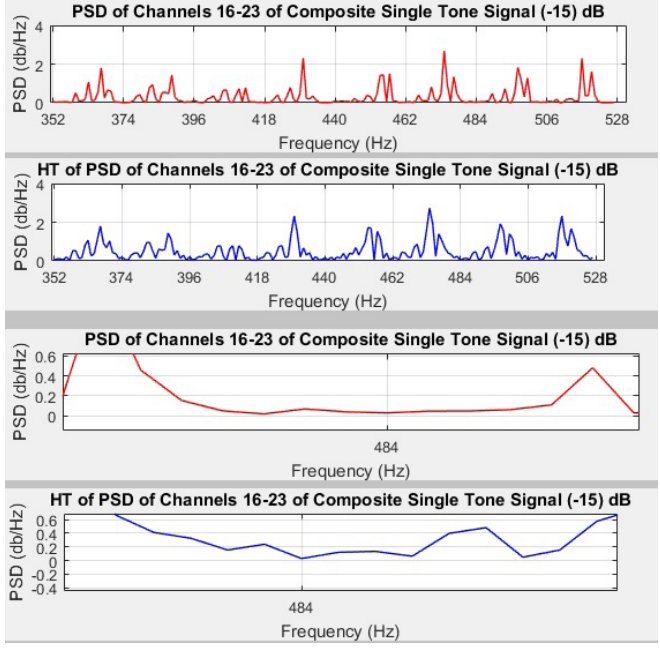

Fig. 11. PSD of channels 16 to 23 at −15 dB, with corresponding Hilbert transform.

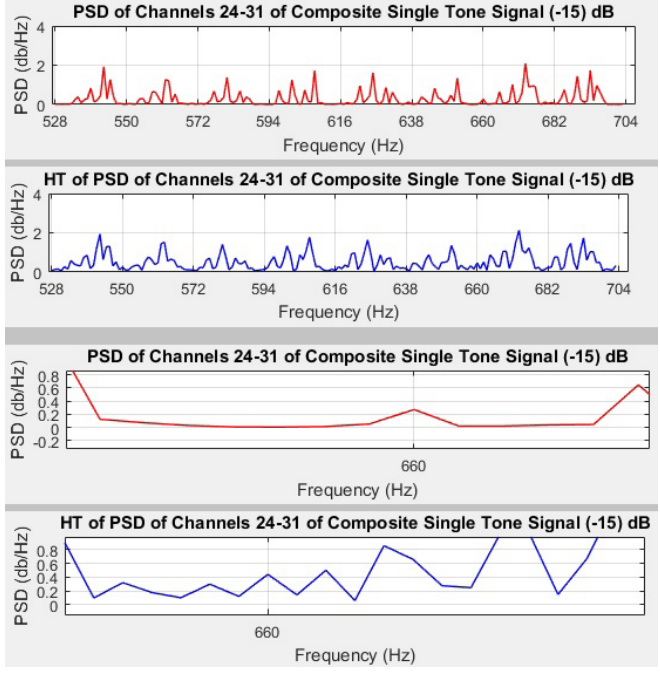

Fig. 12. PSD of channels 24 to 31 at −15 dB, with corresponding Hilbert transform.

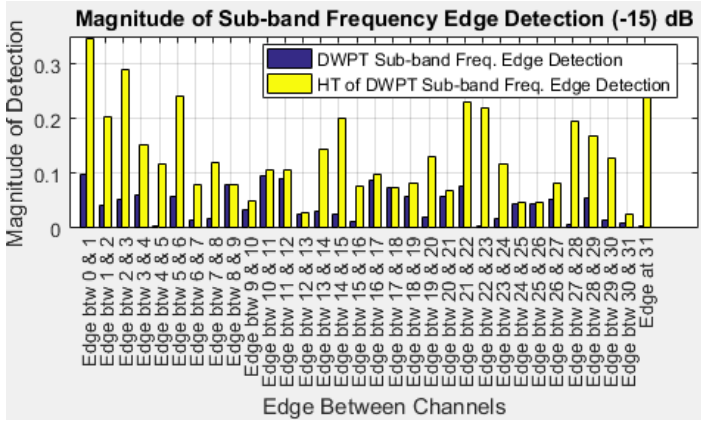

Fig. 13. Magnitude of sub-band frequency edge detection at −15 dB.

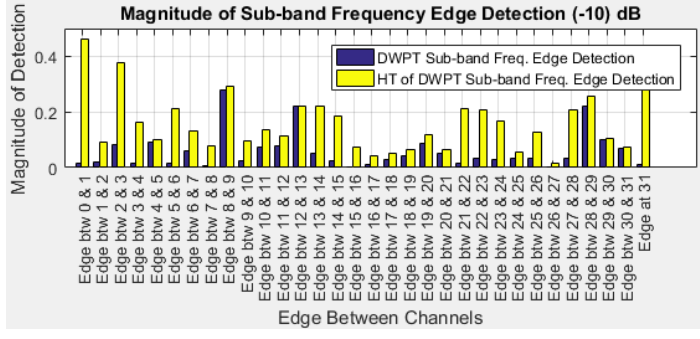

Fig. 14. Magnitude of sub-band frequency edge detection at −10 dB.

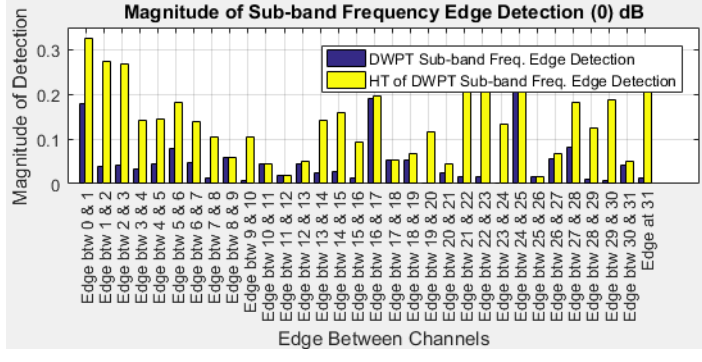

Fig. 15. Magnitude of sub-band frequency edge detection at 0 dB.

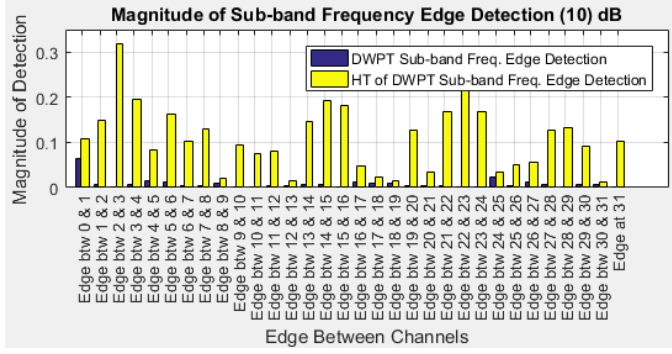

Fig. 16. Magnitude of sub-band frequency edge detection at 10 dB.

the Hilbert transform clearly makes the detection of the sub-band frequency edges better for all the 32 channels under observation.

7. Significance of Result

In the determination of spectrum holes using discrete wavelet packet based spectrum sensing, the accurate identification of the vectors of coefficients in each sub-band plays a very important role in the reliability and accuracy of the spectrum sensing technique. Hence, from the results presented in Sec. 6, the application of the Hilbert transform to a discrete wavelet packet transform (proposed scheme) significantly increases the accuracy in the identification of the vector of coefficients in each sub-band by clearly identifying the edges between each sub-band of the decomposed signal.

Table 2. Comparison of proposed scheme with referred scheme.

	Referred scheme (DWPT without Hilbert transform)	Proposed scheme (DWPT with Hilbert transform)
Strength	* Requires only one transform	* Has higher accuracy than the referred scheme in detection of sub-band edges
Strength	* The use of only one transform makes it a faster technique	* Accuracy of detection remains high as SNR varies
Strength	* Has lower complexity than the proposed scheme	* The Hilbert transform makes it easy to obtain the instantaneous phase of the signal
Weakness	* It is less accurate than the proposed scheme in the detection of sub-band edges	* Has a higher level of complexity due to the combination of two transforms
Weakness	* Accuracy of detection degrades with varying SNR	* The use of two transforms makes it slower than the referred scheme which can be remedied with a fast processor
Weakness	* Absence of the Hilbert transform makes it difficult to obtain the instantaneous phase of a signal	

8. Comparison with Referred Scheme

Like any other technique, the proposed scheme also has its strength and weakness. Table 2 shows the comparison made between the proposed scheme and the referred scheme.

9. Conclusion

In this paper, we presented two transforms: the discrete wavelet packet transform (DWPT) and the Hilbert transform. The method by which the DWPT detects edges in a signal was analyzed by reviewing the Canny edge detector as a local maxima of a wavelet transform modulus. The main objective of the paper which is to achieve an enhanced DWPT sub-band frequency edge detection using Hilbert transform (the proposed scheme) was realized by taking the Hilbert transform of a DWPT decomposed signal. The simulation experiments showed very promising results in that the proposed scheme outperformed the referred scheme (DWPT of a signal) in the detection of the frequency edges in all the sub-band channels of the terminal nodes of the discrete wavelet packet analysis bank shown in Fig. 1 for different values of signal-to-noise ratio. Considering the importance of spectrum sensing in CR implementation and the challenges of existing techniques, the properties of wavelets make it a promising solution to this problem. The improvement in accuracy achieved in this work could be said to outweigh the anticipated delay due to complexity. The reason is that a fast processor can go a long way in reducing the delay.

Acknowledgment

TETFund with Grant Number: TETFUND/FUTMINNA/2017/B/04.

References

1. S. Aditi, Survey paper on Hilbert transform with its application in signal processing, *Int. J. Comput. Sci. Inf. Technol.* **5**(3) (2014) 3880–3882.
2. A. Akulova, A. Fedotov and S. Akulov, Effective QRS-Detector based on Hilbert transform and adaptive thresholding, in *XIV Mediterranean Conf. on Medical and Biological Engineering and Computing*, IFMBE Proceedings, eds. E. Kyriacou, S. Christofides and C. Pattichis, Vol. 57 (Springer, Cham, 2016), pp. 140–144.
3. D. Amit, D. Sheetal and P. Tarnnum, Design and implementation of sobel edge detection technique using VHDL, *Int. J. Adv. Res. Sci. Eng. Techn.* **3**(5) (2016) 2133–2139.
4. S. M. Amrita, A. Ashwini, S. B. Bharya, S. C. Neshwa and S. A. Nitty, Dynamic resolving of edge detection techniques for an image, *Int. J. Innovat. Res. Comput. Commun. Eng.* **4**(3) (2016) 4019–4013.
5. K. Anil and J. Kaur, Evaluating the shortcomings of edge detection operator, *Int. J. Adv. Res. Comput. Sci. Softw. Eng.* **5**(5) (2015) 235–241.
6. G. Baishali and K. Santanu, Analysis of various edge detection methods for X-ray images, in *Int. Conf. Electrical, Electronics, and Optimization Techniques* (ICEET), 3–5 March, (2016), pp. 2694–2699.

7. K. Beant, B. Deepti and R. Suman, Detection of edges using mathematical morphological operators, *Open Trans. Inf. Proc.* **1**(1) (2014) 17–26.
8. J. Canny, A computational approach to edge detection, *IEEE Trans.* **8** (1986) 679–698.
9. S. Cho, J. Heo, G. Jeon, J. Lee, J. Kim, I. Song, G. Tae and Y. Won, *Signals and Systems in MATLAB* (Springer, Berlin, 2009).
10. F. Chu, Z. Peng and P. Tse, A comparison study of improved Hilbert-Huang transform and wavelet transform: Application to fault diagnosis for rolling bearing, *Mech. Syst. Signal Process* **19** (2005) 974–988.
11. L. Cohen, *Time-Frequency Analysis: Theory and Applications* (Prentice Hall, 1995).
12. A. Deshmulch, R. Swati and S. Syed, VHDL based Canny edge detection algorithm, *Int. J. Current Eng. Technol.* **4**(2) (2014) 749–752.
13. E. Guariglia, Entropy and fractal antennas, *Entropy* **18**(3) (2016) 1–17.
14. E. Guariglia, Fractional derivative of the Riemann zeta function, *in Fractional Dynamics*, eds. C. Cattani, H. Srivastava and X. J. Yang (De Gruyter, 2015), pp. 357–368.
15. E. Guariglia, Spectral Analysis of the Weierstrass-Mandelbrot function, IEEE Access (in press), in *Proc. of 2nd International Multidisciplinary Conf. on Computer and Energy Science* (Split, Croatia, 12–14 July, 2017), pp. 1–6.
16. O. Guiherme, D. Korkikian, D. Naccache and P. Rodrigo, Practical instantaneous frequency analysis experiments, in *E-Business and Telecommunications Int. Joint Conf.* (*ICETE*) (Reykjavik Iceland, 29–31 July, 2014), pp. 17–34.
17. S. Haldo and C. Juan, A review of classic edge detectors, *Image Process.* **5** (2015) 90–123.
18. A. Ibrahim, A. Jamil and H. Mahgoub, Gradient based image detection, *Int. J. Eng. Technol.* **8** (3) (2016) 153–156.
19. M. Lakshmanan and H. Nikookar, Construction of optimum wavelet packets for multicarrier based spectrum pooling systems, in *Wireless Pers. Commun.* (2010), pp. 95–121.
20. D. Long, *Comments on Hilbert Transform Based Signal Analysis*, in *All Faculty Publications*, Available at: [http://scholarsarchive.byu.edu/facpub/1312] (2004) Online. Accessed: 11/09/2016.
21. S. Mallat and S. Zhong, Characterization of signals from multiscale edges, *IEEE Trans. Pattern Anal. Mach. Intell.* **14**(7) (1992) 710–732.
22. B. Mantosh and V. G. Vasagari, Rotating kernel transformation based edge detection using adaptive threshold, in *3rd Int. Conf. Electrical, Electronics, Engineering Trends, Communications, Optimization and Sciences* (*EEECOS*) (Tadepalligudem, India, 1–2 June, 2016), pp. 604–609.
23. Mathworks, Wavelet Packets, Online. Available at: [http://www.mathworks.com/help/wavelet/ug/wavelet-packets.html], Accessed: 20/09/2016.
24. C. Nagaraju, K. Pradeep and R. Reddy, Canny edge detection, *Int. J. Eng. Trends Technol.* **X**(Y) (2015) 1–4.
25. G. Pucciarelli, Wavelet analysis in volcanology: The case of Phlegrean fields, *J. Envir. Sci. Eng. A* **6** (2017) 300–307.
26. N. Saravanan, Gear box fault diagnosis using Hilbert transform feature classification by PVSM, *Int. J. Adv. Res. Comput. Sci. Softw. Eng.* **6**(6) (2016) 21–30.
27. M. Sasmita, Comparison study of darker image edges using min-constructor Gaussian operator and traditional operators, *Int. Adv. Res. J. Sci. Eng. Technol.* **2**(3) (2015) 26–28.
28. M. Shaveta and K. Tapas, Comparative analysis of edge detection between gray scale and color image, *Commun. Appl. Elect.* **5**(2) (2016) 38–43.